Biomedical and Pharmaceutical Sciences Faculty Publications

Biomedical and Pharmaceutical Sciences

2003

Equilibrative Nucleoside Transporter Family Members from Leishmania donovani Are Electrogenic Proton Symporters

Alex Stein

Gayatri Vaseduvan

Nicola S. Carter

Buddy Ullman

Scott M. Landfear

See next page for additional authors

Let us know how access to this document benefits you.

Follow this and additional works at: https://scholarworks.umt.edu/biopharm_pubs

Part of the Medical Sciences Commons, and the Pharmacy and Pharmaceutical Sciences Commons

Authors

Alex Stein, Gayatri Vaseduvan, Nicola S. Carter, Buddy Ullman, Scott M. Landfear, and Michael Kavanaugh

Equilibrative Nucleoside Transporter Family Members from *Leishmania donovani* Are Electrogenic Proton Symporters*

Alex Stein‡§, Gayatri Vaseduvan¶, Nicola S. Carter‖, Buddy Ullman‖, Scott M. Landfear ¶, and Michael P. Kavanaugh‡ ‡‡**

From the ‡Vollum Institute and the Departments of ¶Molecular Microbiology and Immunology and ‖Biochemistry and Molecular Biology, Oregon Health & Science University, Portland, Oregon 97239-3098

Leishmania donovani express two members of the equilibrative nucleoside transporter family; LdNT1 encoded by two closely related and linked genes, *LdNT1.1* and *LdNT1.2*, that transport adenosine and pyrimidine nucleosides and LdNT2 that transports inosine and guanosine exclusively. LdNT1.1, LdNT1.2, and LdNT2 have been expressed in *Xenopus laevis* oocytes and found to be electrogenic in the presence of nucleoside ligands for which they mediate transport. Further analysis revealed that ligand uptake and transport currents through LdNT1-type transporters are proton-dependent. In addition to the flux of protons that is coupled to the transport reaction, LdNT1 transporters mediate a variable constitutive proton conductance that is blocked by substrates and dipyridamole. Surprisingly, LdNT1.1 and LdNT1.2 exhibit different electrogenic properties, despite their close sequence homology. This electrophysiological study provides the first demonstration that members of the equilibrative nucleoside transporter family can be electrogenic and establishes that these three permeases, unlike their mammalian counterparts, are probably concentrative rather than facilitative transporters.

Leishmania donovani is a protozoan parasite that causes visceral leishmaniasis, a devastating and often fatal disease in humans. The parasite exhibits a digenetic life cycle; the extracellular, flagellated, and motile promastigote that resides within the insect vector, members of the phlebotomine sandfly family, and the intracellular, aflagellar, and nonmotile amastigote that exists within the phagolysosome of macrophages and other reticuloendothelial cells of the infected mammalian host. The drugs used to treat visceral leishmaniasis have been empirically derived and are toxic, require prolonged and multiple administrations, and are often ineffective. The toxicity can be ascribed to the lack of target specificity within the parasite. Thus, the need for more efficacious and specific drugs is acute.

The design of selective antiparasitic drugs depends on the exploitation of fundamental biochemical differences between parasite and host. Perhaps the most remarkable metabolic discrepancy between protozoan parasites and their human host is that the former are incapable of synthesizing the purine ring *de novo* (1). Thus, all protozoan parasites studied to date have evolved a unique series of purine salvage enzymes that enable parasites to scavenge purines from their host. Purine acquisition by the parasite is initiated by the translocation of extracellular purines across the parasite cell surface membranes, a process that is mediated by nutritionally indispensable nucleoside and nucleobase transporters.

Genetic and biochemical investigations (2, 3) have demonstrated that *L. donovani* express two nucleoside transporter activities of nonoverlapping ligand specificities; LdNT1, which recognizes adenosine and pyrimidine nucleosides, and LdNT2, which mediates the transport of inosine and guanosine. Subsequently, the genes encoding LdNT1 (4) and LdNT2 (5) were isolated by functional rescue of nucleoside transport-deficient *L. donovani*. The LdNT1 locus encompasses two closely related genes, LdNT1.1 and LdNT1.2, and although both are functional after expression in either *Xenopus laevis* oocytes or *L. donovani*, only *LdNT1.1* transcript is detected by Northern blot analysis of promastigote mRNA (6). Predicted amino acid sequences and membrane topologies of LdNT1.1, LdNT1.2, and LdNT2 reveal that all three transporter proteins are members of the equilibrative nucleoside transporter (ENT)[1] family (7). Mammalian cells and other eukaryotes also express a battery of ENTs, as well as sodium-dependent concentrative nucleoside transporters, which are unrelated in sequence to the ENTs (8).

Leishmania parasites maintain a large proton electrochemical gradient across the plasma membrane with a resting potential near −100 mV (9, 10), and it has been conjectured that these organisms generally exploit this electrochemical gradient to drive concentrative uptake of nutrients into the parasite (11). One example of proton driven transport emerged from studies on the proton/*myo*-inositol co-transporter of *L. donovani* (12, 13). In order to determine whether nucleoside uptake into *Leishmania* could utilize this proton gradient, *LdNT1.1*, *LdNT1.2*, and *LdNT2* cRNAs were expressed into *X. laevis* oocytes. Two-electrode voltage clamp measurements on these oocytes revealed that all three carriers were electrogenic. It was further shown that LdNT1.1 and LdNT1.2 mediate two

§ Current address: Dept. of Physiology and Biophysics, University of Washington, Seattle, WA 98195.

** To whom correspondence may be addressed: Dept. of Molecular Microbiology and Immunology, Oregon Health & Science University, Portland, OR 97239-3098. Tel.: 503-494-2426; Fax: 503-494-6862; E-mail: landfear@ohsu.edu.

‡‡ To whom correspondence may be addressed: Center for Structural and Functional Neuroscience, University of Montana, Missoula, MT 59812-1552. Tel.: 406-243-4398; Fax: 406-243-5228; E-mail: Kavanaug@selway.umt.edu.

[1] The abbreviations used are: ENT, equilibrative nucleoside transporter; DPA, dipyridamole; I_{max}, maximum current; pC, picoCoulombs; RMP, resting membrane potential; TMD, transmembrane domain; V_m, membrane potential; V_{max}, maximum transport velocity; V_{rev}, reversal potential; MES, 2-(*N*-morpholino)ethan sulfonic acid.
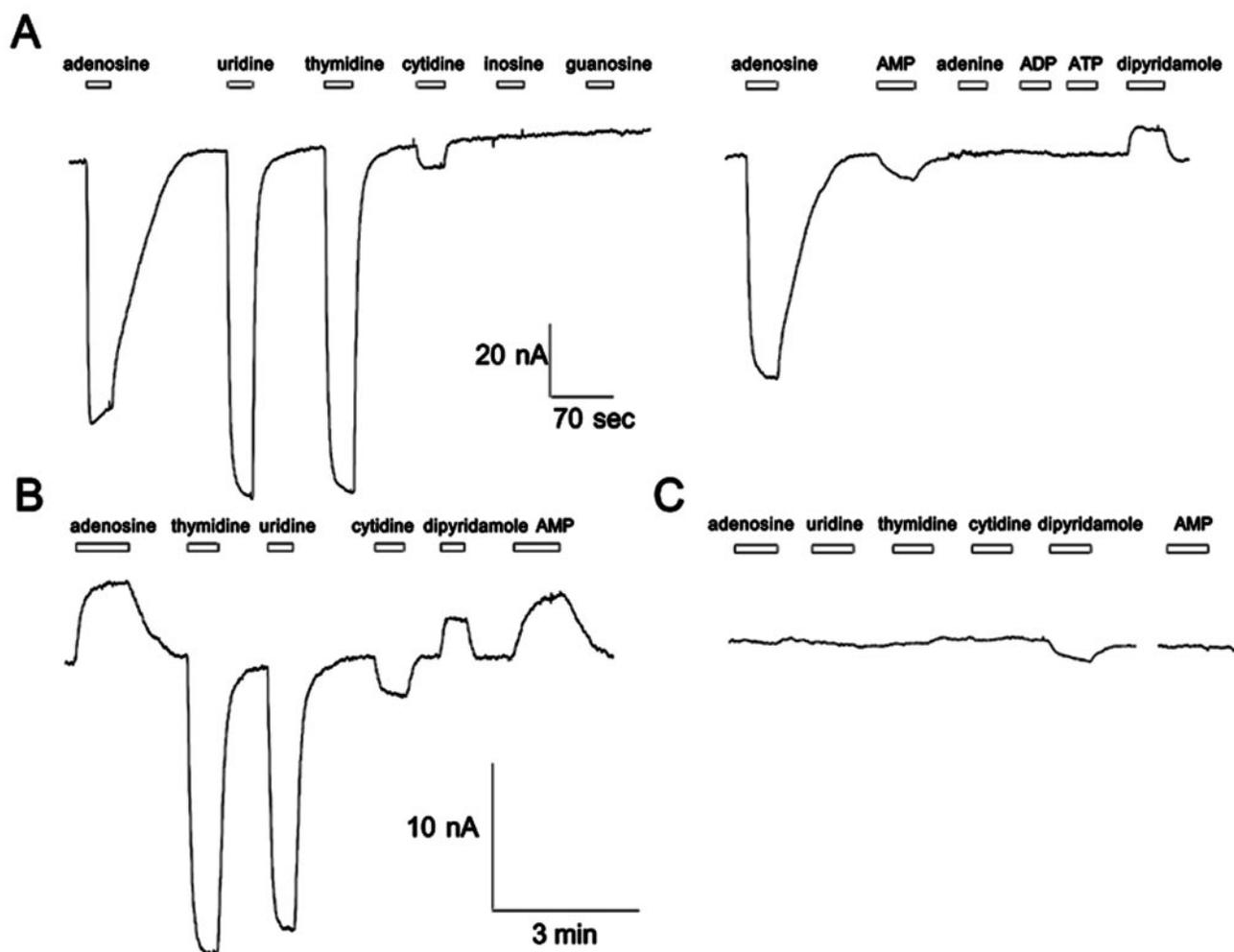
FIG. 1. **Substrate selectivity of the LdNT1 transport system.** Oocytes were voltage-clamped at $V_m = -100$ mV, and substrates (10 μM) of the LdNT1 transport system or other compounds were applied to the bath for the duration indicated by the *bar*. In each case, current recordings from one oocyte are shown, but the experiment was repeated with a total of n oocytes. Currents from oocytes expressing LdNT1.2 (*A*, $n > 6$) and LdNT1.1 (*B*, $n > 6$) or uninjected oocytes (*C*, $n = 5$) are shown. Adenine, inosine, guanosine, ADP, and ATP did not generate a current (*A*) in oocytes injected with *LdNT1.1* or *LdNT1.2* cRNA (data not shown, $n = 4$).

pharmacologically separable ion permeation mechanisms, a proton-dependent, inwardly rectifying transport current, and a tonic, linear, and reversible current carried by protons, respectively. From these results, we conclude that these three nucleoside permeases are likely concentrative proton symporters and that some members of the ENT family are thus active transporters.

<div align="center">EXPERIMENTAL PROCEDURES</div>

Nucleoside Transporter cRNA Expression in Oocytes—Defolliculated stage V-VI *X. laevis* oocytes were microinjected with ~50 ng of capped mRNA that was transcribed with T7 RNA polymerase (Invitrogen) from linearized pL2–5 plasmids (14) containing either *LdNT1.1*, *LdNT1.2*, or *LdNT2* using a nanoliter injector from World Precision Instruments (Sarasota, FL). Oocytes were stored at 16 °C in frog Ringer's solution containing 96 mM NaCl, 2 mM KCl, 1.8 mM CaCl$_2$, 1 mM MgCl$_2$, 5 mM Na-HEPES, pH 7.5, and 1.5% heat-inactivated horse serum. Electrophysiological and radiolabel uptake measurements were performed 4–7 days after cRNA injection.

Electrophysiological Recording—Unless otherwise indicated, recording solutions contained 96 mM NaCl, 2 mM KCl, 1.8 mM CaCl$_2$, 1 mM MgCl$_2$, and a buffer of either 10 mM HEPES-Tris, pH 7.5, 10 mM MES-Tris, pH 5.5, 10 mM MES-Tris, pH 6.5, or 10 mM Tris-HEPES, pH 8.5. In experiments where Na$^+$ was varied or replaced, equimolar concentrations of choline were substituted for the Na$^+$. Two microelectrode voltage-clamp recordings were performed at room temperature using a Gene Clamp 500 interfaced to an IBM compatible PC-AT using a Digidata 1200 A/D controlled by the pCLAMP program suite (version 6.0.3; Axon Instruments). A MacLab/2e analog/digital converter (AD-

Instruments) was used to continuously monitor currents. Microelectrodes were filled with a 3 M KCl solution and had resistances of less than 1.5 MΩ. Substrates and antagonists were introduced by gravity flow into a bath that was continuously perfused with Ringer's solution. Dipyridamole (DPA) was dissolved in 0.1% Me$_2$SO, which did not induce a current itself in either LdNT-injected or uninjected oocytes (data not shown). Current-voltage measurements were made during 250-ms voltage pulses to a series of command potentials. Current data were digitized at 1 kHz. The normalized mean concentration response of currents induced by substrate was fitted by least squares to the Michaelis-Menten equation: $I = I_{max} ([S]/([S] + K_m))$, where S represents either nucleoside or protons. Unless otherwise indicated, K_m values are expressed as mean ± S.E. from fits to individual oocytes. Presteady-state current measurements were recorded at the lowest gain possible to avoid saturation of the amplifier response during the peak of the capacitance transient. For each oocyte, the charge movements carried by the capacitive transient currents were calculated by time integration of the substrate-dependent current after subtraction of steady-state current, which was defined as the current recorded during the last 10 ms of the voltage pulse (16). Charge movements were plotted *versus* voltage and fitted by least squares to the Boltzmann equation: $Q_{tot} = (1 + \exp[e_0 z\delta(V_m - V_{0.5})/kT]) + Q_{offset}$, where Q_{tot} is the total charge movement, $V_{0.5}$ is the midpoint of the charge movement, V_m is the membrane potential, $z\delta$ is the product of the valence of the charge and apparent fraction of the field sensed by that charge, Q_{offset} is the offset that depended on the holding potential, e_0 is the elementary charge, k is the Boltzmann constant, and T is the absolute temperature. For comparisons among oocytes, charge movements were offset vertically by Q_{offset} and normalized to the Q_{tot} in the same oocytes.

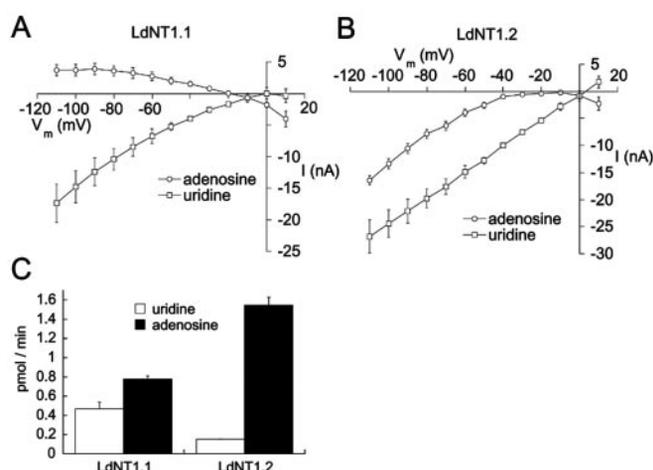*Radiolabeled Nucleoside Flux*—Oocytes expressing *LdNT1.1* or

FIG. 2. **LdNT1.1 and LdNT1.2 exhibit different electrogenic properties.** Currents induced by adenosine and uridine were measured for LdNT1.1 (*A*, *n* = 3) and LdNT1.2 (*B*, *n* = 3). Uptake of [³H]-adenosine and [³H] uridine was also measured over a 30 min time course for LdNT1.1 and LdNT1.2 (*C*, *n* = 5). The uptake observed in LdNT1.1- and LdNT1.2-injected oocytes was between 21- and 177-fold over the background uptake in uninjected oocytes. Data shown are LdNT-specific uptake values.

LdNT1.2 were incubated in wells containing either 10 μM [³H]adenosine or [³H]uridine ($\sim$3 × 10⁻⁵ C$_i$/mmol; Amersham Biosciences) for 30 min. Oocytes were then washed for 20 s with Ringer's buffer, transferred into a scintillation tube, solubilized in 1% SDS, and counted by liquid scintillation spectrometry.

RESULTS

Electrogenic Nucleoside Transport—Inward currents were observed in oocytes that were voltage-clamped at −100 mV and injected with LdNT1.2 cRNA after application of adenosine, AMP, uridine, thymidine, or cytidine at a concentration of 10 μM (Fig. 1*A*). No current was observed when the same concentration of inosine, guanosine, adenine, ADP, or ATP, was added (Fig. 1*A*). In contrast, oocytes microinjected with *LdNT1.1* cRNA exhibited an outward current in response to either adenosine or AMP but an inward current when the pyrimidine nucleosides uridine, cytidine, and thymidine were applied (Fig. 1*B*). No currents were observed in uninjected oocytes in response to the application of any substrate of LdNT1 permeases (Fig. 1*C*). When DPA (0.1% Me₂SO), a potent inhibitor of mammalian nucleoside transporters (7), was superfused over oocytes expressing *LdNT1.1* or *LdNT1.2* cRNA, an outward current similar to that observed with adenosine or AMP for LdNT1.1 was observed (Fig. 1, *A* and *B*). In contrast, DPA application to uninjected oocytes induced a small inward current ($\sim$20% of the outward current observed after injection with *LdNT1.2* cRNA, Fig. 1*B*). In summary, the known substrates of LdNT1.1 and LdNT1.2, as well as AMP and DPA, induced currents in each permease.

Although LdNT1.1 and LdNT1.2 differ in sequence by only 6 residues (4), an interesting distinction in the adenosine and AMP response currents of these two transporters was observed. At V_m = −100 mV, adenosine and AMP generate outward currents similar to that observed with DPA when applied to LdNT1.1 (Fig. 1*B*). In LdNT1.2, however, a significant inward current developed in response to 10 μM adenosine and AMP (Fig. 1*A*). In order to correlate the differences in the electrical properties of LdNT1.1 and LdNT1.2 with the potential function of these proteins as concentrative transporters, the elicited current was plotted as a function of voltage (I/V curves) for oocytes superfused with either 10 μM adenosine or uridine (Fig. 2). The adenosine-dependent currents for LdNT1.1 were outward at hyperpolarized membrane potentials, reversed at a

membrane potential of $\sim$−20 mV, and were inward at depolarized potentials (Fig. 2*A*), whereas the adenosine currents mediated by LdNT1.2 were inwardly rectifying (Fig. 2*B*). However, the shape of the LdNT1.2 current *versus* voltage curve for adenosine exhibited a negative slope conductance at membrane potentials more positive than V_m = −10 mV. In contrast, 10 μM uridine triggered inward currents in both LdNT1.1 and LdNT1.2.

The data in Fig. 2 were used to estimate molar charge to substrate flux ratios for the two transporters. First, uptake of [³H]adenosine and [³H]uridine over a 30 min time course was measured for each permease using 5 oocytes (Fig. 2*C*). Using the average resting membrane potential (RMP) measured for these oocytes (LdNT1.1: RMP = −53.0 ± 5.0 mV; LdNT1.2: RMP = −27.0 ± 0.6 mV), the integrated charge crossing the membrane over the 30 min time course of the uptake assay was calculated from the currents in the same group of oocytes defined at each RMP by the curves in Fig. 2, *A* and *B*. The molar amounts of charge thus calculated were divided by the molar amounts of radiolabeled ligand that crossed the membrane during the 30 min assay to estimate the charge to substrate flux ratios. According to these calculations, LdNT1.1 countertransported 0.029 charges per molecule of adenosine and cotransported 0.13 charges per molecule of uridine. LdNT1.2 co-transported 0.0035 charges per molecule of adenosine and co-transported 0.46 charges per molecule of uridine. These non-integer charge to flux values clearly indicate that substrate flux is not tightly coupled to the total currents mediated by LdNT1 transporters. An explanation for charge to flux ratios significantly below unity is offered under "Discussion." However, the charge to flux ratio of 0.46 for the uridine-induced currents in LdNT1.2 suggests that there is a substantial coupling of transmembrane charge movement to substrate import.

pH Dependence of Adenosine-induced Steady-state Currents—To further investigate the origin of the currents observed in Figs. 1 and 2, and to determine whether they might represent proton symport, the pH dependence of the steady-state adenosine-response currents was examined for LdNT1.1 and LdNT1.2. Oocytes expressing each permease were exposed to voltage jumps from a holding potential of −60 mV to a range of command potentials. Currents elicited in the absence of adenosine were then subtracted from those recorded in the presence of 30 μM adenosine, resulting in the current *versus* time traces shown in Fig. 3*A*. At pH 6.5, 7.5, and 8.5 LdNT1.1 and LdNT1.2-expressing oocytes revealed an initial transient capacitive or presteady-state current that then decayed to a steady-state value. No currents were observed in uninjected oocytes (data not shown, *n* > 5).

The steady-state adenosine response currents for LdNT1.2 were plotted as a current-voltage curve (Fig. 3*B*). Adenosine induced an inward rectifying current at pH 6.5, which is consistent with an inward flux of protons that is coupled to import of adenosine. Notably, the currents at pH 7.5 and 8.5 were considerably smaller than at pH 6.5, again consistent with a coupled flux of protons that experiences a smaller driving force at increased external pH values. There were some differences however in the shapes of the curves, with negative slope conductances at positive potentials at both pH 7.5 and 8.5.

In contrast, the shapes of the steady-state current-voltage curves for LdNT1.1 (Fig. 3*C*) were more complex than those for LdNT1.2. One notable difference between the two permeases is that the adenosine-elicited currents for LdNT1.1 generally exhibited negative slope conductances and reversal potentials that were shifted $\sim$25 mV per unit change in external pH, in contrast to LdNT1.2. These data suggest that a primary action of adenosine in LdNT1.1 is to block a membrane conductance
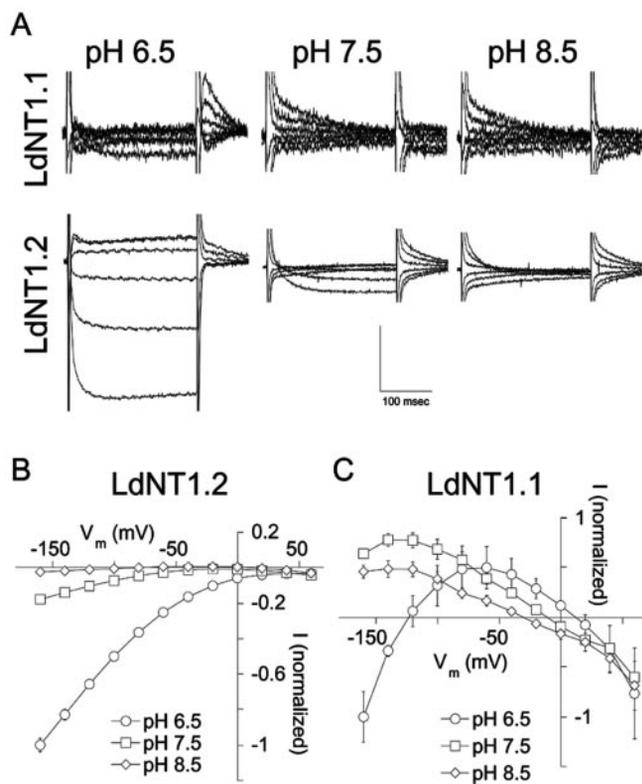
FIG. 3. **pH dependence of adenosine transport currents in LdNT1.1 and LdNT1.2.** Oocytes expressing LdNT1.1 and LdNT1.2 were voltage-clamped, and 30 μM adenosine was applied to the bath at pH 6.5, 7.5, and 8.5. Voltage steps were executed from a holding potential of -60 mV to between $+60$ and -160 mV, and currents obtained in the absence of adenosine were subtracted from currents recorded in the presence of adenosine. *A*, representative families of adenosine response currents at membrane potentials between $+60$ and -140 mV are shown. Records of LdNT1.1 were low-pass filtered at 500 Hz. LdNT1.2 records were digitized at 1 kHz. The vertical scale bar is 100 nA for LdNT1.1 and 400 nA for LdNT1.2. No adenosine response currents were observed in uninjected oocytes ($n > 6$). The current-voltage relationships of the LdNT1.2 (*B*) and LdNT1.1 (*C*) adenosine response currents at pH 6.5, 7.5, and 8.5 were plotted. Data represents normalized mean $\pm$ S.E. ($n = 3$–4).

FIG. 4. **LdNT transporters are proton- but not sodium-dependent.** *A*, different concentrations of adenosine were applied to voltage-clamped oocytes expressing LdNT1.2 at pH 6.5, 7.5, and 8.5. Adenosine dose responses at $V_m = -100$ mV are shown; curves are least squares fits of the data (normalized mean $\pm$ S.E., $n = 4$–5) to the Michaelis-Menten equation with K_m values of 2.63 ± 0.45 μM (pH 6.5), 1.00 ± 0.09 μM (pH 7.5), and 0.50 ± 0.08 μM (pH 8.5). *B*, [³H]adenosine uptake in oocytes expressing LdNT1.1 and LdNT1.2 was not significantly different when sodium was completely replaced with choline during the assay ($n = 5$). *C*, LdNT1.2 adenosine dose responses at $V_m = -100$ mV in sodium and choline-substituted recording solutions are shown; curves are least squares fits of the data (normalized mean $\pm$ S.E., $n = 3$) to the Michaelis-Menten equation with K_m values of 0.999 ± 0.09 μM (Na⁺), 1.09 ± 0.06 μM (choline+). The dose response in choline was fitted with an normalized I_{max} of 1.1 ± 0.1.

that is carried in part by protons. It is notable that in contrast to the results at higher pH values, the outward current induced by LdNT1.1 at pH 6.5 decreased again at potentials more negative that -60 mV and again became inward at potentials more negative than ~ -120 mV, resulting in an inverted U-shaped curve (Fig. 3*C*). These results suggest that at low pH, LdNT1.1, like LdNT1.2, mediates an adenosine-coupled proton symport process that gives rise to an inward current. This substrate-coupled import of protons would be of the largest magnitude at pH 6.5 and at the most polarized membrane potentials, as demonstrated in Fig. 3*B* for the corresponding current for LdNT1.2. The inverted U-shaped curve for LdNT1.1 at pH 6.5 could thus be explained by the additive combination of the blockage of a proton leak current by adenosine, which predominates above a membrane potential of -60 mV, and an adenosine-coupled proton symport current that becomes apparent below a membrane potential of -60 mV.

To further define the proton dependence of LdNT1.2 steady-state currents, the adenosine concentration dependence of these response currents was examined at $V_m = -100$ mV and at pH 6.5, 7.5, and 8.5 (Fig 4*A*). The magnitudes of the currents elicited by adenosine concentrations ranging from 0.1–100 μM adenosine were greatest at pH 6.5 and lowest at pH 8.5. The transporter affinity decreased and the maximal transport rate increased with increasing proton concentrations. Thus from the
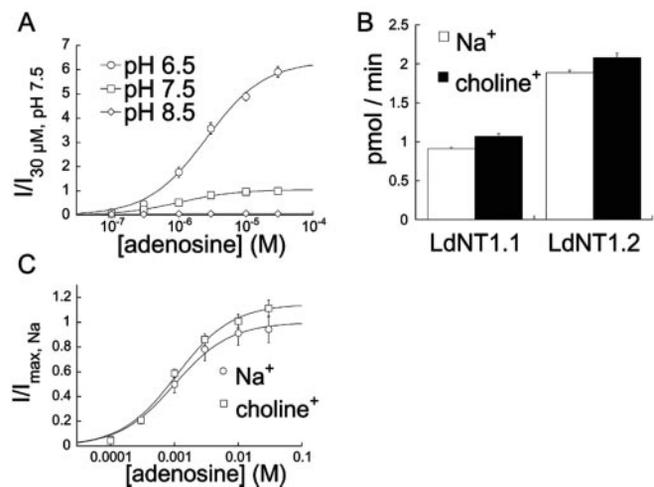
currents observed, a K_m value of 1.00 ± 0.09 μM could be calculated for LdNT1.2 at pH 7.5. At pH 6.5, the transporter exhibited a K_m value of 2.63 ± 0.45 μM and an I_{max} of $600 \pm 26\%$ greater than the I_{max} at pH 7.5. At pH 8.5, the K_m was 0.50 ± 0.08 μM, and the I_{max} was $5.2 \pm 0.5\%$ of its value at pH 7.5. In summary, the increase of adenosine-elicited currents in LdNT1.2 at lower pH values further supports proton symport as a mechanism for transport.

Lack of Sodium Dependence of Adenosine Uptake or Adenosine-induced Currents—The observation of electrogenic transport for these protozoan nucleoside permeases contrasts with other members of the ENT family, which are equilibrative permeases and not electrogenic (7). In contrast another family of nucleoside transporters, the CNTs, are sodium-dependent electrogenic active transporters (15). Consequently, whether LdNT1.1- or LdNT1.2-mediated adenosine uptake might be sodium dependent was also determined. Replacement of sodium in the bath with equimolar choline did not significantly affect either LdNT1.1- or LdNT1.2-mediated adenosine uptake (Fig. 4*B*). Furthermore, the LdNT1.2 transporter exhibited no significant difference in either the affinity or maximal current when sodium was replaced with choline (Fig. 4*C*). Indeed, replacement of sodium with choline did not affect adenosine-induced currents for LdNT1.2 at any adenosine concentration, indicating that LdNT1.2 is not a sodium symporter.

Capacitive Gating Currents—As noted above (Fig. 3), application of voltage jumps to oocytes expressing LdNT1.1 or LdNT1.2 induced adenosine-dependent presteady-state or transient currents that decayed with exponential time constants of <100 msec. For some transporters, such transient currents have been linked to binding of a co-transported ion to the permease (16). To determine whether the adenosine-induced transient currents could be explained by binding of protons to the permeases, and could thus be useful for probing interaction of protons with the transporters, the kinetic properties of these pre-steady-state currents were examined at sev-
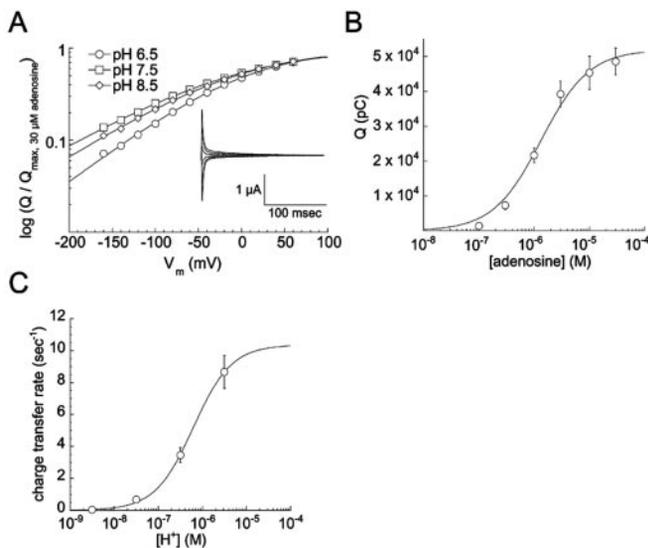
FIG. 5. **Kinetics of the transient current blocked by adenosine transport in LdNT1.2.** *A*, a family of subtracted current records in a representative LdNT1.2-expressing oocyte showing the voltage dependence of the capacitative transient current induced by 30 μM adenosine at pH 7.5 is shown (*inset*). A voltage command pulse to -60 mV was executed from a 0.250 s pre-pulse of from $+60$ to -160 mV (20-mV increments). Integrated charge movements from cells expressing LdNT1.2 at pH 6.5, 7.5, and 8.5 were normalized to the Q_{tot} and fitted by least squares to a Boltzmann function ($n = 5$). *B*, the adenosine concentration dependence of the integrated charge movements was fitted to the Michaelis-Menten equation with a K_m of 1.35 ± 0.11 μM. *C*, the charge transfer rate of the LdNT1.2 transporter was calculated by adjusting the Q_{tot} by zδ, and then dividing the steady-state current induced by 30 μM adenosine at $V_m = -100$ mV by the adjusted Q_{tot}. The proton concentration dependence of the charge transfer rate was fitted to the Michaelis-Menten equation with a K_m of 0.62 ± 0.05 μM and V_{max} of 10.36 ± 0.23 per second.

eral proton concentrations by time integration of the currents following the return of the clamped membrane to the holding potential from a voltage step (Fig. 5). The transient charge movement obeyed similar voltage dependences at pH 6.5, 7.5, and 8.5 (Fig. 5*A*, $n = 4$). The total charge movement induced by adenosine was similar at these pHs (Q_{tot} (pH 6.5) is 35033 $\pm$ 3980 pC; Q_{tot} (pH 7.5) is 44771 $\pm$ 2883 pC; Q_{tot} (pH 8.5) is 39179 $\pm$ 1771 pC). The midpoint of the integrated current voltage dependence is a measurement of the transporter's affinity for the translocated charge (16). The midpoint of the integrated transient current mediated by 30 μM adenosine was also found to be essentially independent of pH ($V_{0.5}$ (pH 6.5) is 3.31 $\pm$ 3.23 mV; $V_{0.5}$ (pH 7.5) is -9.53 ± 3.33 mV; $V_{0.5}$ (pH 8.5) is -4.93 ± 2.53 mV). The transient current elicited by 30 μM adenosine also exhibited a similar slope to its voltage dependence at the three pHs examined, which implies that the translocated charge experiences the same fraction of the membrane electric field under these conditions (slope (pH 6.5) is 60.90 $\pm$ 2.70 mV^{-1}; slope (pH 7.5) is 81.88 $\pm$ 3.59 mV^{-1}; slope (pH 8.5) is 74.40 $\pm$ 4.00 mV^{-1}) (17). The insensitivity of midpoint and slope values to changes in pH implies that the capacitive transient current is not due to a proton binding event. Rather, it may be a charge-moving conformational change in the transport protein.

To verify that the transient current elicited by adenosine was associated with transporter function, the adenosine concentration dependence of the integrated capacitive current was examined (Fig. 5*B*). The magnitude of the capacitive current was dependent upon adenosine concentration in a dose-dependent manner, and the apparent affinity of the transporter for adenosine (K_m is 1.35 $\pm$ 0.11 μM) when measured in this way was similar to that derived from analysis of the steady-state cur-
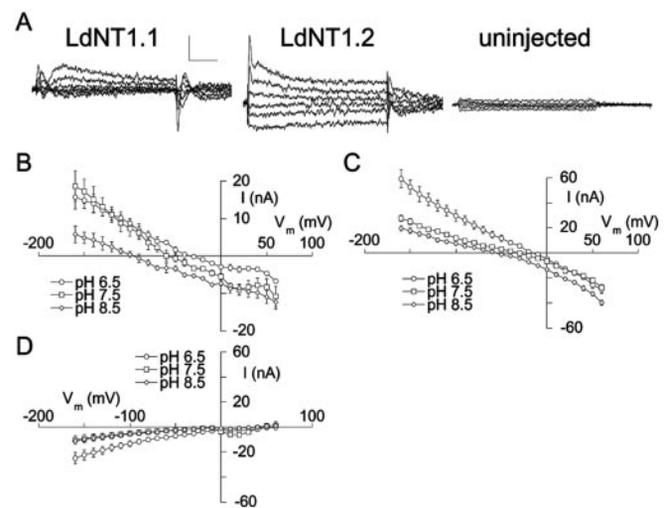

FIG. 6. **DPA blocks a proton leak in LdNT1.1 and LdNT1.2.** 30 μM DPA was applied to oocytes expressing LdNT1.1 or LdNT1.2, and uninjected oocytes at pH 6.5, 7.5, and 8.5. *A*, representative current families of the DPA response current at pH 7.5 are shown. Cells were voltage-clamped at -50 mV, and the membrane potential was stepped to between $+60$ and -140 mV. Data are subtractions of control currents from currents recorded during dipyridamole application. *B*, current-voltage relations for the LdNT1.1-mediated current induced by dipyridamole at pH 6.5, 7.5, and 8.5 are shown. The reversal potential (V_{rev}) of the response current is pH-dependent ($n = 3$). $V_{rev} = -35 \pm 6$ mV (pH 6.5), -55 ± 8 mV (pH 7.5), -96 ± 7 mV (pH 8.5). *C*, current-voltage relations for LdTN1.2-mediated currents ($n = 3$). $V_{rev} = -16 \pm 3$ mV (pH 6.5), -34 ± 3 mV (pH 7.5), -57 ± 3 mV (pH 8.5). *D*, DPA response currents in uninjected oocytes ($n = 3$).

rents (K_m is 1.00 $\pm$ 0.09 μM, Fig. 4). These results imply that the pre-steady-state currents reflect transporter function.

It is possible to estimate the charge transfer rate of the transporter by dividing the steady-state current through the transporter (I, pC/sec) by the total number of elementary charges blocked by adenosine (Q/zδ, pC) and assuming a charge to flux stoichiometry of 1:1 (16). The charge transfer rate was calculated at pHs between 5.5 and 8.5 (Fig. 5*C*). Performing this calculation at pH 7.5 revealed that the transporter moves 0.7 $\pm$ 0.05 times per second through the membrane at -100 mV. The proton dose dependence of the transporter's charge transfer rate was fitted with a proton affinity of 0.62 $\pm$ 0.05 μM, and the maximal cycling rate was found to be 10.4 $\pm$ 0.2 per sec.

DPA Blocks a Tonic Proton Leak through LdNT1 Transporters—DPA is a high affinity antagonist of mammalian adenosine transporters (7) but does not significantly inhibit nucleoside transporters from parasitic protozoa (1). Despite its failure to significantly inhibit the *Leishmania* permeases, DPA activates a current in LdNT-expressing oocytes (Fig. 1, *A* and *B*). To further characterize the effect of DPA on these transporters, the transmembrane currents recorded prior to DPA application were subtracted from currents recorded during DPA application revealing a current in LdNT1-expressing cells that was not observed in uninjected oocytes (Fig. 6*A*). The DPA-induced currents in LdNT1.1 and LdNT1.2 were linear and reversible, and they were outward at more negative membrane potentials (Fig. 6, *B* and *C*). The LdNT1-mediated currents saturated with respect to the DPA concentration (K_m is 35 $\pm$ 10 μM in LdNT1.2 at $V_m = -100$ mV; data not shown, $n = 4$). In contrast, the smaller current that was present in uninjected oocytes was inward and did not reverse (Fig. 6*D*),

Similar to the behavior of the transporter current blocked by adenosine, the reversal potential of the DPA-elicited currents was observed to shift to more positive values as the extracellular concentration of protons was increased, suggesting that
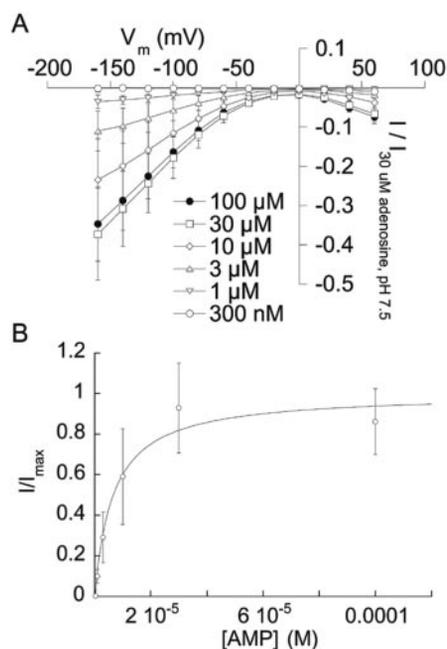
FIG. 7. **Kinetics of AMP transport in LdNT1.2.** Oocytes expressing LdNT1.2 were voltage-clamped, and different concentrations of adenosine 5′-monophosphate were superfused into the recording chamber. *A*, the response currents at each voltage and at different concentrations of AMP were plotted ($n = 3$). *B*, at -100 mV, the concentration dependence of the current response was fitted to the Michaelis-Menten equation with a K_m of 9.1 ± 3.2 μM. Data represent normalized mean $\pm$ S.E.

this current is carried substantially by protons (Fig. 6, *B* and *C*). A quantitative analysis of the reversal potential pH dependence is precluded by the DPA-induced current in uninjected oocytes (Fig. 6*D*).

AMP Induces Currents for LdNT1.1 and LdNT1.2—The observation that AMP was able to elicit currents in oocytes microinjected with either *LdNT1.1* or *LdNT1.2* cRNA (Fig. 1) was surprising in view of the negative charge of the nucleotide and the fact that nucleotides typically are not taken up by intact eukaryotic cells. To further investigate this phenomenon, we measured current-voltage curves for AMP-induced currents for LdNT1.2 (Fig. 7), the permease that elicited inward directed currents with this ligand. For LdNT1.2 the maximal AMP-induced current at $V_m = -100$ mV was 20.1% of the maximal current induced by a saturating (30 μM) concentration of adenosine in the same oocytes (Fig. 7*A*). The AMP response current in LdNT1.2 was saturable with respect to AMP, and its concentration dependence exhibited an apparent affinity of 9 ± 3 μM (Fig. 7*B*). The shapes of the AMP and adenosine response current-voltage relationships are qualitatively similar at pH 7.5 (compare Fig. 7*A* to Fig. 3*B*). It does not appear that the AMP-induced current could be ascribed to adenosine contamination because the purity of the AMP was verified by high performance liquid and thin layer chromatography (data not shown). Furthermore, when [³H]AMP was applied to LdNT1.2-expressing oocytes, the radiolabel was taken up robustly by the oocytes, but no significant amount of [³H]adenosine was liberated into the supernatant.[2] Hence, the AMP-induced currents cannot be ascribed to hydrolysis of AMP that liberates free adenosine into the medium followed by uptake of this liberated adenosine by the permease. The origin of these AMP-induced currents is currently under investigation.

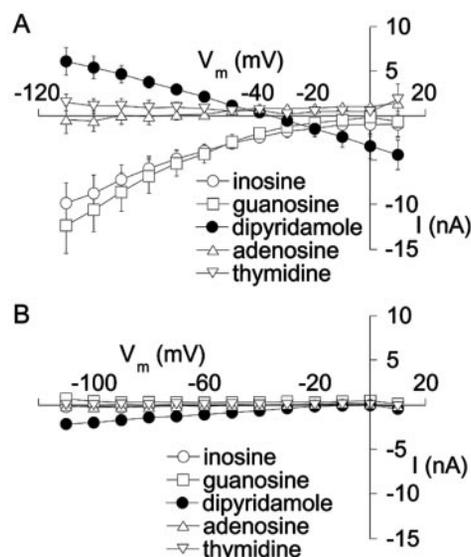*The LdNT2 Inosine-Guanosine Permease Is Also Electro-*

---

[2] S. M. Landfear, unpublished data.

FIG. 8. **Electrogenic nucleoside transport in LdNT2.** Nucleosides and DPA were bath-applied to voltage-clamped LdNT2-expressing (*A*) and uninjected (*B*) oocytes at a concentration of 10 μM. Steps of the membrane potential to between $+10$ and -110 mV were executed, and the currents elicited at each voltage are indicated. Data are represented as mean $\pm$ S.E. ($n = 4$).

genic—The other nucleoside transporter of *L. donovani*, LdNT2, mediates the uptake of inosine and guanosine, is also a member of the ENT family, and exhibits 33% sequence identity to LdNT1.1 (5). Oocytes injected with *LdNT2* cRNA were also shown to elicit inward response currents to the application of ligands. Inosine and guanosine, but not adenosine or thymidine, mediated inward rectifying currents in a voltage-dependent fashion (Fig. 8*A*). LdNT2 also mediated a reversible DPA-induced outward current at negative membrane potentials, similar to that observed for LdNT1.1 and LdNT1.2. Neither inosine, guanosine, adenosine, nor thymidine induced a current in uninjected oocytes, although 10 μM DPA elicited a small inward current (Fig. 8*B*). The induction of inward rectifying currents specifically by substrates of the LdNT2 permease implies that this transporter also couples the symport of protons to nucleosides, much as demonstrated above for the LdNT1.2 carrier. The outward directed currents elicited by DPA suggest that this compound blocks a constitutive leak current in LdNT2, in a manner similar to that observed for LdNT1.1 and LdNT1.2 (Fig. 6).

DISCUSSION

We have shown that adenosine/pyrimidine nucleoside transport through the LdNT1 transporters is associated with the activation of transmembrane currents. The magnitudes of the currents mediated by LdNT1.2 and the substrate fluxes mediated by both LdNT1.1 and LdNT1.2 were dependent on the proton, but not the sodium, gradient, strongly suggesting that these proteins are proton/nucleoside symporters. Unlike the *Leishmania* proton/*myo*-inositol symporter MIT, which transports *myo*-inositol with a charge to flux ratio of 1 (13), LdNT1 did not mediate substrate flux that was tightly coupled to total charge translocation. Although LdNT1.1 and LdNT1.2 are very similar in sequence, they exhibit striking differences with respect to their electrogenic properties, most notably that adenosine strongly blocks a leak current in LdNT1.1, whereas adenosine induces an inward proton current in LdNT1.2. It is likely that the adenosine blockage of the leak current in LdNT1.1 obscures an inward directed adenosine-coupled proton current similar to that observed in LdNT1.2. In fact, the inward directed current observed for LdNT1.1 at pH 6.5 below a trans-

membrane voltage of -120 mV (Fig. 3*C*) is likely to be such a transport-coupled current that overcomes the block of the leak current at this lower pH value and more negative membrane potential. Thus the essential difference between the two permeases may be that adenosine effects a more robust block of the leak current in LdNT1.1 compared with LdNT1.2.

We have also shown that LdNT1 transporters mediate a constitutive proton conductance that is blocked by the compound DPA. Unlike the mammalian ENTs, the *Leishmania* nucleoside transporters are not significantly inhibited by DPA at concentrations that obliterate transport by mammalian ENTs (2), and thus the precise nature of the interaction between this compound and the LdNTs is not clear. Nonetheless the ability of DPA, which is very lipophilic and known to affect the entry of many structurally unrelated compounds into mammalian cells (18, 19), to block the constitutive proton leak is instructive, as it likely reflects a similar block of this leak current that is induced by interaction of substrates with the LdNT1 permeases.

We hypothesize that part of the reason charge translocation appears to be loosely coupled to substrate flux in LdNT1.1 and LdNT1.2 is that adenosine transport blocks the constitutive proton conductance in a similar manner to DPA. By summing a linear current with a pH-dependent reversal potential such as the one observed upon application of DPA (Fig. 6, *B* and *C*) and a pH-dependent inwardly rectifying transport current such as that observed after application of adenosine to LdNT1.2 at pH 6.5 (Fig. 3*B*), it is possible to generate current-voltage curves with shapes corresponding to the adenosine response current-voltage curves. This hypothesis is supported by the observation that, while lower pH increases the relative contribution of inward adenosine response current at negative potentials in LdNT1.1, it also shifts the reversal potential of the current-voltage curve to more positive potentials (Fig. 3*C*), as would be expected for a current that represents blockage of a proton leak. The presence of this blocked proton conductance would cause our calculations of the charge to flux ratio to be significant underestimates of the actual value, especially when the measurements are made at the resting potentials of the oocytes (between -53 and -27 mV) rather than at highly polarized membrane potentials that favor the influx of protons that are coupled to adenosine transport. In summary, the blockage of a constitutive proton leak by substrates complicates the estimation of charge to substrate flux ratios for these protozoan nucleoside transporters. However, this constitutive leak is blocked less efficiently in LdNT1.2 than in LdNT1.1, and uridine blocks this leak less effectively in both transporters compared with adenosine (Fig. 2). Consequently, the charge to flux ratio calculated for uridine in LdNT1.2 (0.46 charges per molecule) is probably the estimate that most closely reflects the value for proton symport coupled to a substrate. Hence, substrates appear to mediate the import of at least ~ 0.5 charge units per molecule.

LdNT1.1 and LdNT1.2 differ by only 6 amino acid residues in sequence, and three of these polymorphisms are located on the extreme COOH termini of the proteins. Despite the high degree of identity, these transporters exhibit different affinities for the substrates adenosine and uridine (4) and mediate different currents during adenosine and AMP transport. The COOH-terminal residues are the uncharged ATY in LdNT1.1 compared with the highly charged ERH in LdNT1.2. While these sequences could be important in determining the distinct electrogenic properties of the proteins, perhaps a more likely residue for the observed differences is P43 in LdNT1.1. This proline is a serine in LdNT1.2, and it is the only polymorphism that lies within a predicted transmembrane domain (TMD1). The other polymorphisms include M107I (between TMD2 and TMD3) and T160A (between TMD4 and TMD5), which are located within predicted hydrophilic loops of the permeases. Mutational analysis outside the scope of this manuscript will be needed to evaluate the role of each polymorphism on the kinetic and electrophysiological differences between LdNT1.1 and LdNT1.2.

Our analysis of the transporters responsible for nucleoside transport in *L. donovani*, LdNT1.1, LdNT1.2, and LdNT2, has demonstrated that these proteins couple the large proton electrochemical gradient available to the parasites to nucleoside uptake. Purine uptake is vital to the survival of the parasites, as they are incapable of purine biosynthesis, and the ability of the parasite to concentrate essential purines from the extracellular medium may thus provide an evolutionary advantage by promoting its survival within both the insect vector and/or the vertebrate host. The parasite nucleoside transporters studied here exhibit $\sim 30\%$ identity at the amino acid sequence level with members of the mammalian equilibrative nucleoside transporter family. Since LdNT1.1, LdNT1.2 and LdNT2 are apparently proton symporters, it now appears that some members of the ENT family are concentrative permeases. This conclusion is also consistent with previous studies performed on transport of nucleosides by intact procyclic forms of the related protozoan *Trypanosoma brucei*, in which the dependence of nucleoside transport upon the proton electrochemical gradient across the parasite plasma membrane strongly suggested proton symport as a mechanism of active transport (20). Similar studies in which the ENT1 (*At*) permease from *Arabidopsis thaliana* was expressed in yeast also strongly suggest that this permease is a proton symporter (21). It is possible that relatively few changes in amino acid sequence determine whether a nucleoside transporter of this family functions as a concentrative or equilibrative permease. However, the extensive differences in sequence between equilibrative and concentrative members of the ENT family make it difficult to predict which residues may be required for proton symport and suggest that extensive structure-function studies will likely be required to elucidate determinants of active transport.

The ability of the nucleotide AMP to induce currents in LdNT1.1 and LdNT1.2 that are very similar to those induced by adenosine, as well as the ability of radiolabel from [^{3}H]AMP to enter LdNT1.1 or LdNT1.2-expressing oocytes, is intriguing, as these anionic metabolites are thought not to be transported across the plasma membranes of eukaryotic cells. We are currently pursuing further studies to determine the nature of the interaction of AMP with the LdNT1.1 and LdNT1.2 permeases.

REFERENCES

1. Carter, N. S., Rager, N., and Ullman, B. (2003) in *Molecular and Medical Parasitology* (Marr, J. J., Nilsen, T., and Komuniecki, R., eds) pp. 197–223, Academic Press, London
2. Aronow, B., Kaur, K., McCartan, K., and Ullman, B. (1987) *Mol. Biochem. Parasitol.* **22,** 29–37
3. Iovannisci, D. M., Kaur, K., Young, L., and Ullman, B. (1984) *Mol. Cell. Biol.* **4,** 1013–1019
4. Vasudevan, G., Carter, N. S., Drew, M. E., Beverley, S. M., Sanchez, M. A., Seyfang, A., Ullman, B., and Landfear, S. M. (1998) *Proc. Natl. Acad. Sci. U. S. A.* **95,** 9873–9878
5. Carter, N. S., Drew, M. E., Sanchez, M., Vasudevan, G., Landfear, S. M., and Ullman, B. (2000) *J. Biol. Chem.* **275,** 20935–20941
6. Vasudevan, G., Ullman, B., and Landfear, S. M. (2001) *Proc. Natl. Acad. Sci. U. S. A.* **98,** 6092–6097
7. Hyde, R. J., Cass, C. E., Young, J. D., and Baldwin, S. A. (2001) *Mol. Membrane Biol.* **18,** 53–63
8. Baldwin, S. A., Mackey, J. R., Cass, C. E., and Young, J. D. (1999) *Mol. Med. Today* **5,** 216–224
9. Zilberstein, D., Philosoph, H., and Gepstein, A. (1989) *Mol. Biochem. Parasitol.* **36,** 109–118
10. Vieira, L., Slotik, I., and Cabantchik, Z. I. (1995) *J. Biol. Chem.* **270,** 5299–5304
11. Zilberstein, D. (1993) *Adv. Parasitol.* **32,** 261–291
12. Drew, M. E., Langford, C. K., Klamo, E. M., Russell, D. G., Kavanaugh, M. P., and Landfear, S. M. (1995) *Mol. Cell. Biol.* **15,** 5508–5515

13. Klamo, E. M., Drew, M. E., Landfear, S. M., and Kavanaugh, M. P. (1996) *J. Biol. Chem.* **271,** 14937–14943
14. Arriza, J. L., Kavanaugh, M. P., Fairman, W. A., Wu, Y.-N., Murdoch, G. H., North, R. A., and Amara, S. G. (1993) *J. Biol. Chem.* **268,** 15329–15332
15. Yao, S. Y., Ng, A. M., Loewen, S. K., Cass, C. E., Baldwin, S. A., and Young, J. D. (2002) *Am. J. Physiol. Cell Physiol.* **283,** C155–168
16. Wadiche, J. I., Arriza, J. L., Amara, S. G., and Kavanaugh, M. P. (1995) *Neuron* **14,** 1019–1027
17. Woodhull, A. M. (1973) *J. Gen. Physiol.* **61,** 687–708
18. Kessel, D., and Dodd, D. C. (1972) *Biochim. Biophys. Acta* **288,** 190–194
19. Graff, J. C., Wohlhueter, R. M., and Plagemann, P. G. (1977) *J. Biol. Chem.* **252,** 4185–4190
20. de Koning, H. P., Watson, C. J., and Jarvis, S. M. (1998) *J. Biol. Chem.* **273,** 9486–9494
21. Möhlmann, T., Mezher, Z., Schwerdtfeger, G., and Neuhaus, H. E. (2001) *FEBS Lett.* **509,** 370–374